Published in "Physical Review A 83(6): 062703, 2011"
which should be cited to refer to this work.

Absolute angle-differential elastic cross sections for electron collisions with diacetylene

M. Allan
Department of Chemistry, University of Fribourg, chemin du Musée 9, CH-1700 Fribourg, Switzerland

C. Winstead and V. McKoy
A. A. Noyes Laboratory of Chemical Physics, California Institute of Technology, Pasadena, California 91125, USA

We report measured and calculated differential elastic cross sections for collisions of low-energy electrons with diacetylene (1,3-butadiyne). A generally satisfactory agreement between theory and experiment has been found. The calculated cross sections provide interesting insight into the underlying resonant structure.

I. INTRODUCTION

Electron collisions with diacetylene (1,3-butadiyne, H−C≡C−C≡C−H) are relevant in a number of practical environments. Diacetylene is a potential precursor (at least in the laboratory) for the H−C≡C−C≡C$^-$ anion that has been recently detected in interstellar space [1,2]. Diacetylene has also been detected in the upper layers of planetary atmospheres (Titan, Uranus) [3,4], where free electrons occur. It may also be an intermediate in dust formation in technological plasmas [5,6] and is known to be an intermediate in the formation of soot in flames [7–9]. Diacetylene is furthermore an interesting molecule in being carbon- and energy-rich, as well as a relatively long linear molecule.

These considerations motivated our earlier study of absolute dissociative electron attachment (DEA) cross sections [10] and of vibrational excitation cross sections of this molecule [11]. Here we report measured and calculated elastic cross sections that might serve as inputs to plasma simulations. A comparison of the measured cross sections to those from calculations, which provide the contributions of individual symmetries, offers valuable insight into the underlying scattering mechanisms and resonant structure.

II. METHODS

A. Experiment

The measurements were performed using a spectrometer with hemispherical analyzers [12–15]. The energy resolution was about 15 meV in the energy-loss mode, at a beam current of around 200 pA. The instrumental response function was determined on elastic scattering in helium and all spectra were corrected as described earlier [13,15]. Absolute values of the cross sections were determined by the relative flow technique as described by Nickel *et al.* [16] using the calculated helium elastic cross sections of Nesbet [17] as a reference. The confidence limit is about ±20% for the elastic cross sections (two standard deviations).

The angular distributions were measured using a combination of mechanical setting of the analyzer and magnetic deflection with a magnetic angle changer [18,19]. The curves were corrected for the instrumental response function and fitted to the absolute values measured at discrete angles of 20°, 45°, 90°, 135°, and 180°, as described in Refs. [13,15]. The angle of the magnetic scan was incremented in steps of 2.5°. Further details of the experiment can be found in the paper on vibrational excitation [11].

B. Theory

The equilibrium geometry of diacetylene was optimized using second-order Möller-Plesset perturbation theory within the 6-31G(d) Gaussian basis set as defined in the electronic structure program GAMESS [20], resulting in a C–H bond length of 1.0672 Å and lengths of 1.3745 and 1.2246 Å, respectively, for the single and triple C–C bonds. For comparison, measured values are 1.09 Å for the C–H bond length and 1.384 and 1.218 Å, respectively, for the lengths of the single and triple C–C bonds [21].

Electron-scattering calculations were carried out at the optimized geometry using a massively parallel implementation of the Schwinger multichannel (SMC) variational method [22–24]. The one-electron space used in the calculations was constructed along the same lines as that used in earlier work on ethylene [25,26]. It comprised the contracted Gaussian basis set denoted 6–311++G(2d,2p) in standard notation, again as defined in GAMESS, together with a supplement of uncontracted s-type Gaussians (exponent 0.036) distributed around the molecule on a rectangular grid with spacing 2.3 Å. (This value was erroneously given as 2.3 bohr in Ref. [25].) In the present case the grid was extended to ±6.9 Å in the direction of the molecular axis while keeping the perpendicular dimensions at ±4.6 Å, as in the ethylene calculations. Grid points at the origin and at ±2.3 Å along the molecular axis were omitted. The purpose of this supplement is to improve the representation of the scattering wave function by expanding the computational "box" covered by the basis set in a way that allows oscillations, and thus to improve the description of weaker collisions at large impact parameter. After dropping the $x^2 + y^2 + z^2$ linear combination of Cartesian d orbitals and excluding three linear combinations to avoid numerical linear dependence, the resulting one-electron basis set contained 332 functions.

Within this one-electron set, the target ground state was described at the single-configuration self-consistent-field (SCF) level. The SCF virtual orbitals were subjected to an orthogonal transformation to form modified virtual orbitals (MVOs) [27] defined by an 8 + cationic Fock operator constructed from the occupied SCF orbitals, in order to obtain a set of compact virtuals for the representation of target polarization [25]. That representation included singlet-coupled virtual excitations of

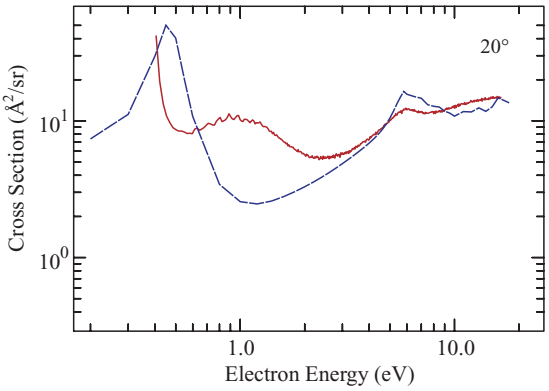

FIG. 1. (Color online) Elastic cross sections at 20°. Solid (red) line, experiment; dashed (blue) line, theory.

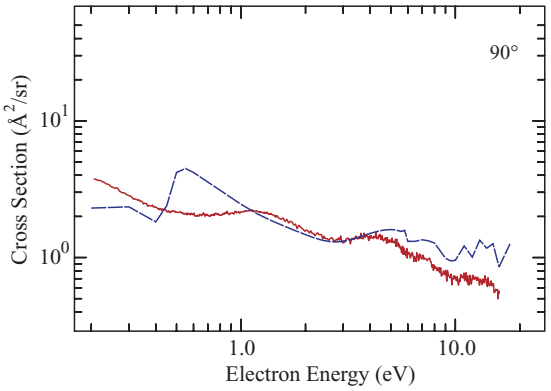

FIG. 3. (Color online) Elastic cross sections at 90°.

the target from all nine valence orbitals into the lowest 30 MVOs, as well as triplet-coupled excitations from the π_u and π_g occupied valence orbitals into each of the two MVOs that closely resembled the π_g^* and π_u^* virtual valence orbitals. To each such target configuration, we coupled all of the MVOs to form an $(N+1)$-particle doublet configuration space in which to carry out the SMC calculation. Configurations with an MVO coupled to the unexcited target were of course also included. Separate scattering calculations were carried out for the eight irreducible representations of the D_{2h} subgroup of the full $D_{\infty h}$ point group. The number of configurations in a given representation varied from 11 166 in ^2A_g to 9 438 in ^2A_u, with a total of 82 129 over all eight representations. The arbitrary cutoff at 30 in the size of the particle space used to represent polarization resulted in the number of b_{2u} and b_{3u} orbitals included in the calculation differing by 1. This difference provided a partial convergence check on the final results in that the cross sections for degenerate representations ($^2B_{2u}$ and $^2B_{3u}$, $^2B_{2g}$ and $^2B_{3g}$) did indeed turn out to be nearly identical (see Fig. 6) except at discrete points, all but one of them in the energy range above 10 eV where pseudoresonances affect the cross section.

III. RESULTS AND DISCUSSION

The elastic cross sections are shown as a function of energy for five representative angles in Figs. 1–5. The vertical scales of all five figures are the same to facilitate comparison between them. In the experimental data the $^2\Pi_u$ resonance near 1 eV, with its narrow boomerang structure [11,28], clearly influences the elastic cross sections in the 0.5–1.5 eV energy range. The $^2\Pi_g$ resonance around 5.5 eV causes a broad hump in the 4–7 eV region. The shape and peak energy vary strongly with the scattering angle, indicating an angle-dependent coherent superposition with a nonresonant background.

The $^2\Pi_u$ resonance is too sharp in the calculated data, as expected for a fixed-nuclei calculation, but it is also too low in energy (about 0.47 eV instead of 1 eV), probably indicating that the scattering wave function is "overcorrelated" relative to the Hartree-Fock wave function used to define the target molecule. We observed similar overcorrelation of the lowest-energy π^* resonance in pyrazine [29] when we included triplet-coupled excitations necessary to describe the highest-energy π^* resonance. The calculated fixed-nuclei width of about 65 meV, obtained from a fit to the eigenphase sum, is qualitatively compatible with the width of 30 meV derived from the width of the narrowest boomerang structures [11].

The calculated position of the $^2\Pi_g$ resonance, on the other hand, is close to where it is observed experimentally, though this may in part reflect cancellation of errors (overcorrelation versus channel coupling). At higher energies we see the usual pseudoresonances. Qualitatively, the calculation reproduces correctly the height and the shape of the structure due to the $^2\Pi_g$ resonance, superimposed on the nonresonant background, for the various scattering angles.

Figure 6 shows the contributions of the different symmetries to the calculated integral cross section and provides interesting

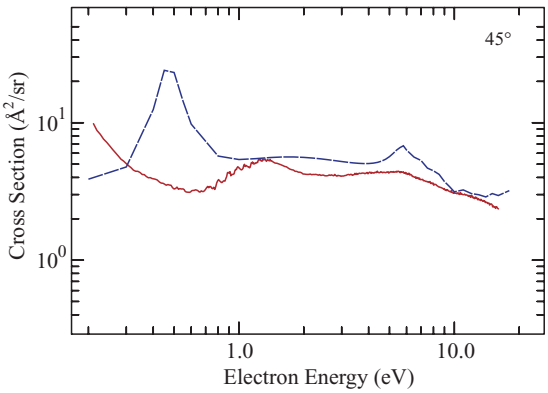

FIG. 2. (Color online) Elastic cross sections at 45°.

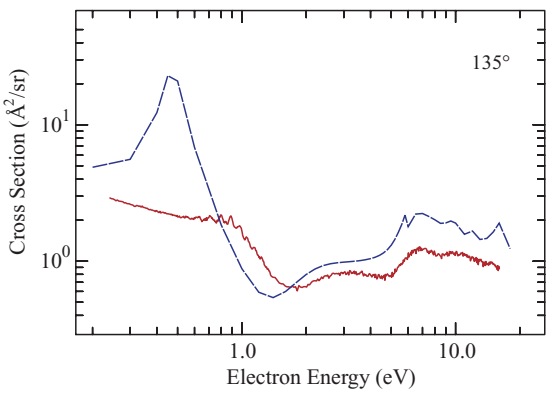

FIG. 4. (Color online) Elastic cross sections at 135°.

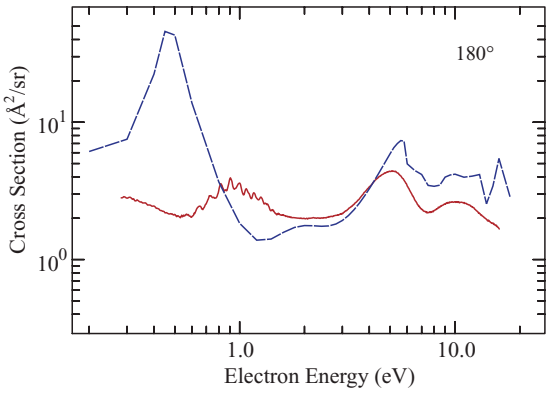

FIG. 5. (Color online) Elastic cross sections at 180°.

insight into the resonant structure and the origin of the various features. There appears to be a Ramsauer minimum in the ^2A_g ($^2\Sigma_g$) component, although in the experiment this would be completely obscured by the (nonresonant) maximum in $^2B_{1u}$ ($^2\Sigma_u$). The sudden drop in the $^2B_{1u}$ contribution near 9 eV is associated with a jump in the eigenphase sum, so it appears to be a shape resonance with an unusual profile. Being rather weak, it does not much affect the differential cross sections, although it may account for dips near 9 eV in the differential cross sections at 90° and 135° (Figs. 3 and 4). In ^2A_g, there is a resonance with a Fano-type profile near 5.9 eV that might be a real Feshbach resonance or just a pseudoresonance; it is difficult to say from this level of calculation. We point out that such a resonance is expected in this energy range in view of the 10.15 eV ionization energy (leading to a $^2\Pi_g$ cation) of diacetylene ([30] and references therein). Sharp Feshbach resonances were observed at 6.7, 6.8, and 7.0 eV in the yield of slow electrons [31]. A more diffuse core excited resonance was postulated to be at the origin of the 5.25 eV dissociative electron attachment band [11,32]. A broad (width $\approx$ 2 eV) shape resonance was postulated experimentally at 4.3 eV, based on enhancement of the C–H stretch vibration, and assigned as $^2\Sigma_u$ (or $^2\Sigma_g$) [11]. Somewhat surprisingly,

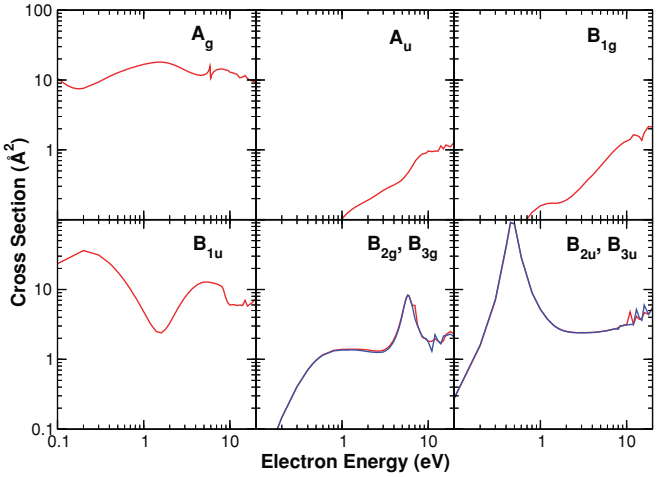

FIG. 6. (Color online) Contributions of different irreducible representations of the D_{2h} subgroup to the calculated integral elastic cross section. The last two panels on the bottom row contain two curves, which at most energies coincide within the width of the lines.

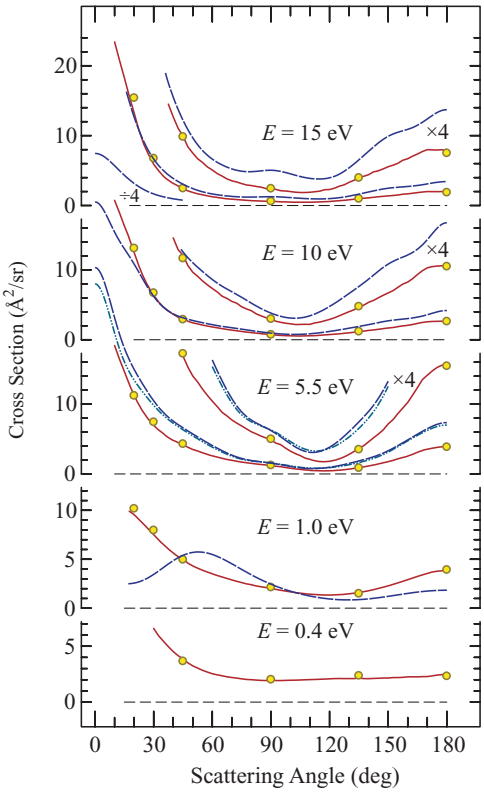

FIG. 7. (Color online) Angular distributions of the elastic cross sections. Yellow circles indicate individual absolute measurements by the relative flow method, the continuous (red) line is the result of a magnetic angle scan, in steps of 2.5°. The dashed (blue) lines are the theoretical results at the same energy except at 5.5 eV, where calculated results at 5.4 eV (dash-dotted cyan lines) and 5.6 eV (dashed blue lines) are shown.

there is no indication of such a resonance in the B_{1u} (Σ_u) or A_g (Σ_g) contribution in Fig. 6.

The angular distributions are shown in Fig. 7. The agreement between theory and experiment is generally satisfactory. As already mentioned, the present calculation puts the $^2\Pi_u$ resonance at about 0.47 eV, while the fixed-nuclei approximation makes it very narrow, causing the calculated cross section at 0.45 eV to be artificially high. The calculated cross section at 0.4 eV is therefore not shown in the figure. The agreement is better at 1 eV, where a substantial difference is found only below 50°. The general shape above 50°, with a minimum around 120°, is well reproduced. At 5.5, 10, and 15 eV the agreement is very good in the forward hemisphere, while the calculated values are somewhat higher than experiment in the backward hemisphere. The experimental integral and momentum-transfer cross sections determined from the angular distributions (with visual extrapolation down to 0°) are given, and compared with theory, in Table I and Fig. 8. As mentioned previously, the $^2\Pi_u$ resonance is calculated to lie at about 0.45 eV and makes the theoretical value at 0.4 eV too large. The same problem occurs to a lesser degree for the $^2\Pi_g$ resonance at 5.5 eV. The remaining cross sections agree very reasonably, although the tendency of the calculated differential cross sections to exceed the measured values in the backward hemisphere, already noted above, causes the

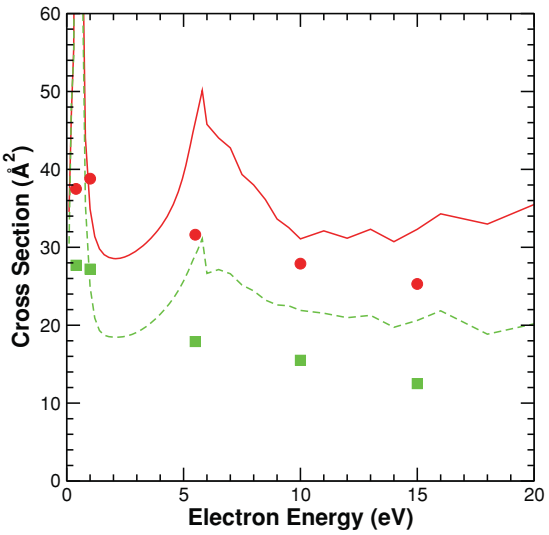

FIG. 8. (Color online) Measured (red circles) and calculated (red solid curve) integral elastic cross sections, along with the measured (green squares) and calculated (green dashed curve) momentum-transfer cross sections.

calculated integral and momentum-transfer cross sections to exceed the experimental values at most energies.

As discussed previously [32], the $^2\Pi_g$ shape resonance at 5.5 eV can mix with $(\pi_g,\pi_u^{*2})\,^2\Pi_g$ core-excited terms associated with the $(\pi_g \rightarrow \pi_u^*)\,^1\Delta_u$ state, whose vertical excitation energy is 5.3 eV [31]. Such mixing provides a pathway for the resonance to decay into the $^1\Delta_u$ state. The same type of mechanism may also promote decay of the resonance into other open $\pi_g \rightarrow \pi_u$ channels, including $^3\Sigma_u^+$, $^3\Delta_u$, $^3\Sigma_u^-$, and $^1\Sigma_u^-$ [31,33]. Although the SMC calculations take account of such channel mixing, our method of solving for the scattering amplitude does not generate wave functions from which we might gauge its significance. As a diagnostic, therefore, we performed a configuration-interaction calculation on the $^2\Pi_g$ anion within a small active space comprising π_u, π_g, σ_u^*, π_u^*, and π_g^* valence orbitals. The $\pi_u^4\pi_g^4\pi_g^*$ configuration has a coefficient of 0.91 in the resulting wave function, suggesting that channel mixing is in fact likely to be weak in this case.

TABLE I. Integral (ICS) and momentum-transfer (MTCS) elastic cross sections (Å^2).

E (eV)	0.4	1.0	5.5	10.0	15.0
Experimental ICS	37.5	38.8	31.6	27.9	25.3
Theoretical ICS	117.4	34.9	47.3[a]	31.1	32.3
Experimental MTCS	27.7	27.2	17.9	15.5	12.5
Theoretical MTCS	110.2	24.9	28.4[a]	21.9	20.6

[a]Theoretical value at 5.4 eV.

IV. SUMMARY

We have reported experimental and computational results for elastic collisions of low-energy electrons with diacetylene. As expected from a consideration of the unoccupied valence orbitals, the cross section is dominated by $^2\Pi_u$ and $^2\Pi_g$ shape resonances. The former appears in the measured cross sections at about 1.0 eV, while the calculation places it about 0.5 eV lower, indicating that the scattering wave function, which includes configurations built on excited states of the target in order to describe polarization effects, is overcorrelated relative to the single-configuration description of the neutral molecule. On the other hand, the measured and computed energies of the $^2\Pi_g$ resonance agree fairly well. There is, likewise, reasonable agreement between the measured and calculated results for the angle-dependent cross sections, except in the immediate vicinity of the $^2\Pi_u$ resonance.

ACKNOWLEDGMENTS

We thank Professor John P. Maier and Jacques Lecoultre for a generous sample of diacetylene. The research of M.A. is part of Project No. 200020-131962/1 of the Swiss National Science Foundation, of project SBF No. C07.0018 of the State Secretariat for Education and Research, and of COST Action CM0601. The work of V.M. and C.W. was supported by the Chemical Sciences, Geosciences, and Biosciences Division, Office of Basic Energy Sciences, Office of Science, US Department of Energy under Grant No. DE-FG02-97ER14814 and employed the facilities of the Supercomputing and Visualization Facility at the Jet Propulsion Laboratory.

[1] J. Cernicharo, M. Guelin, M. Agundez, K. Kawaguchi, M. McCarthy, and P. Thaddeus, Astron. Astrophys. **467**, L37 (2007).
[2] H. Gupta, S. Brünken, F. Tamassia, C. A. Gottlieb, M. C. McCarthy, and P. Thaddeus, Astrophys. J. **655**, L57 (2007).
[3] D. E. Shemansky, A. I. F. Stewart, R. A. West, L. W. Esposito, J. T. Hallett, and X. Liu, Science **308**, 978 (2005).
[4] M. Burgdorf, G. Orton, J. van Cleve, V. Meadows, and J. Houck, Icarus **184**, 634 (2006).
[5] J. Benedikt, A. Consoli, M. Schulze, and A. von Keudell, J. Phys. Chem. A **111**, 10453 (2007).
[6] M. Mao, J. Benedikt, A. Consoli, and A. Bogaerts, J. Phys. D **41**, 225201 (2008).
[7] X. Gu, Y. Guo, A. M. Mebel, and R. I. Kaiser, J. Phys. Chem. A **110**, 11265 (2006).
[8] X. Gu, Y. Guo, A. M. Mebel, and R. I. Kaiser, Combust. Flame **151**, 245 (2007).
[9] A. DAnna, M. Alfe, B. Apicella, A. Tregrossi, and A. Ciajolo, Energy Fuels **21**, 2655 (2007).
[10] O. May, J. Fedor, B. C. Ibănescu, and M. Allan, Phys. Rev. A **77**, 040701(R) (2008).
[11] M. Allan, O. May, J. Fedor, B. C. Ibănescu, and L. Andric, Phys. Rev. A **83**, 052701 (2011).
[12] M. Allan, J. Phys. B **25**, 1559 (1992).
[13] M. Allan, J. Phys. B **38**, 3655 (2005).
[14] M. Allan, J. Phys. B **40**, 3531 (2007).
[15] M. Allan, Phys. Rev. A **81**, 042706 (2010).

[16] J. C. Nickel, P. W. Zetner, G. Shen, and S. Trajmar, J. Phys. E **22**, 730 (1989).
[17] R. K. Nesbet, Phys. Rev. A **20**, 58 (1979).
[18] F. H. Read and J. M. Channing, Rev. Sci. Instrum. **67**, 2373 (1996).
[19] M. Zubek, N. Gulley, G. C. King, and F. H. Read, J. Phys. B **29**, L239 (1996).
[20] M. W. Schmidt *et al.*, J. Comput. Chem. **14**, 1347 (1993).
[21] D. R. Lide, ed., *CRC Handbook of Chemistry and Physics*, 90th ed. (CRC Press, Boca Raton, 2009), pp. 9–33.
[22] K. Takatsuka and V. McKoy, Phys. Rev. A **24**, 2473 (1981).
[23] K. Takatsuka and V. McKoy, Phys. Rev. A **30**, 1734 (1984).
[24] C. Winstead and V. McKoy, Comput. Phys. Commun. **128**, 386 (2000).
[25] C. Winstead, V. McKoy, and M. H. F. Bettega, Phys. Rev. A **72**, 042721/1 (2005).
[26] M. Allan, C. Winstead, and V. McKoy, Phys. Rev. A **77**, 042715 (2008).
[27] C. W. Bauschlicher, J. Chem. Phys. **72**, 880 (1980).
[28] M. Allan, Chem. Phys. **86**, 303 (1984).
[29] C. Winstead and V. McKoy, Phys. Rev. A **76**, 012712 (2007).
[30] M. Allan, E. Kloster-Jensen, and J. P. Maier, Chem. Phys. **17**, 11 (1976).
[31] M. Allan, J. Chem. Phys. **80**, 6020 (1984).
[32] O. May, J. Fedor, B. C. Ibănescu, and M. Allan, Phys. Rev. A **77**, 040701(R) (2008).
[33] F. Vila, P. Borowski, and K. D. Jordan, J. Phys. Chem. A **104**, 9009 (2000).